Chemical Geology 339 (2013) 52–60

Contents lists available at SciVerse ScienceDirect

Chemical Geology

journal homepage: www.elsevier.com/locate/chemgeo

CO_2 output discharged from Stromboli Island (Italy)

S. Inguaggiato [a,b,*], M.P. Jácome Paz [b], A. Mazot [c], H. Delgado Granados [b], C. Inguaggiato [d], F. Vita [a]

[a] Istituto Nazionale di Geofisica e Vulcanologia, Sezione di Palermo, via Ugo La Malfa, 143, 90145 Palermo, Italy
[b] Instituto de Geofísica, Universidad Nacional Autónoma de México, Ciudad Universitaria, Coyoacán 04510, México, D. F., Mexico
[c] GNS Science Wairakei Research Centre, 114 Karetoto Road, Wairakei, Private Bag 2000, Taupo, New Zealand
[d] Università di Palermo, Palermo Italy

ARTICLE INFO

Article history:
Accepted 3 October 2012
Available online 13 October 2012

Keywords:
CO_2 flux
CO_2 output
Stromboli Island
SO_2 flux

ABSTRACT

Total CO_2 output from soil gas and plume, discharged from the Stromboli Island, was estimated. The CO_2 emission of the plume emitted from the active crater was estimated on the basis of the SO_2 crater output and C/S ratio, while CO_2 discharged through diffuse soil emission was quantified on the basis of 419 measurements of CO_2 fluxes from the soil of the whole island, performed by using the accumulation chamber method. The results indicate an overall output of ≅416 t day^{-1} of CO_2 from the island. The main contribution to the total CO_2 output comes from the summit area (396 t day^{-1}), with 370 t/day from the active crater and 26 t day^{-1} from the Pizzo sopra La Fossa soil degassing area. The release of CO_2 from peripheral areas is ≅20 t day^{-1} by soil degassing (Scari area mainly). The result of the soil degassing survey confirms the persistence of the highest CO_2 degassing areas located on the North-East crater side and Scari area.

1. Introduction

Stromboli, the northernmost island of the Aeolian arc in the southern Tyrrhenian Sea, represents the subaerial part of a large edifice extending from a depth of about 2500 m to 924 m a.s.l. The emerged part of the volcano formed in the last 100 Ka through alternation of lava effusions and explosive eruptions, from vents mostly located on a NE–SW fracture system. In the last 13 Ka the magma became more basic, with a shoshonitic basaltic composition (Francalanci et al., 1989; Pasquarè et al., 1993 and references therein). The persistent mildly explosive activity, characteristic of Stromboli (e.g. "Strombolian" activity) probably began between the third and the seventh centuries A.D. and continued without significant interruption or modifications until present time (Rosi et al., 2000).

The typical strombolian activity occurs from three main craters aligned NE–SW and located in the upper part of the Sciara del Fuoco activity consists of intermittent explosions, usually at intervals of 10–20 min, throwing glowing scoriae, ash and solid blocks to heights of less than a few hundreds of meters. This normal activity is episodically interrupted by lava effusions and by more violent explosions, called "major explosions" and "paroxysms" by Barberi et al. (1993).

Occasionally, about 2 or 3 times a year a major explosion occurs with jets at over 500 m and launching blocks. Most explosive eruptions of Stromboli are called paroxysms, throwing blocks that reach above 1000 m and can generate small pyroclastic flows and ash across the island; these events could generate avalanches towards the Sciara del Fuoco and sometimes tsunamis (Bertagnini et al., 2008).

The last recent effusive eruptions occurred in 2002–2003 and 2007 (Inguaggiato et al., 2011a).

The main shallow fluids manifestations of the Stromboli volcano are characterized by:

- Continuous gas plume emitted from Stromboli craters, with an output of 6000 to 12,000 tons/day depending on the level of activity. Water vapor is the main component of the plume (over 60 wt.%) followed by CO_2, SO_2 with minor HCl and HF (Allard et al., 1994; Burton et al., 2007).
- Soil CO_2 degassing occurring in the summit (North-East crater area mainly) and peripheral areas (Scari area mainly) (Carapezza and Federico, 2000; Brusca et al., 2004).
- Carbon and Helium rich thermal wells (up to 42 °C) located in the Stromboli village area. These thermal waters suggest relevant inputs of magmatic gas into the shallow aquifer on the basis of the amount and the isotope composition of Carbon and Helium with a clear magmatic origin (Carapezza et al., 2004; Inguaggiato and Rizzo, 2004; Capasso et al., 2005; Inguaggiato et al., 2011a,b).

In Stromboli volcano many studies of soil CO_2 diffuse emission have been carried out and 2 high permeability areas have been located (Carapezza and Federico, 2000; Brusca et al., 2004; Carapezza et al., 2004). Two fixed monitoring soil stations was installed in these anomalous degassing areas (STR01 and STR02; Fig. 1). STR02 was installed at the summit of the volcano in the Pizzo La Fossa area, in the NE climb to the crater while STR01 were installed in a small area in the Scari village (Brusca et al., 2004; Rizzo et al., 2009; Inguaggiato et al., 2011a). These continuous monitoring stations represent the geochemical network system of soil degassing utilized for a

* Corresponding author at: Istituto Nazionale di Geofisica e Vulcanologia, Sezione di Palermo, via Ugo La Malfa, 143, 90145 Palermo, Italy.
E-mail address: s.inguaggiato@pa.ingv.it (S. Inguaggiato).

0009-2541/$ – see front matter © 2012 Elsevier B.V. All rights reserved.
http://dx.doi.org/10.1016/j.chemgeo.2012.10.008

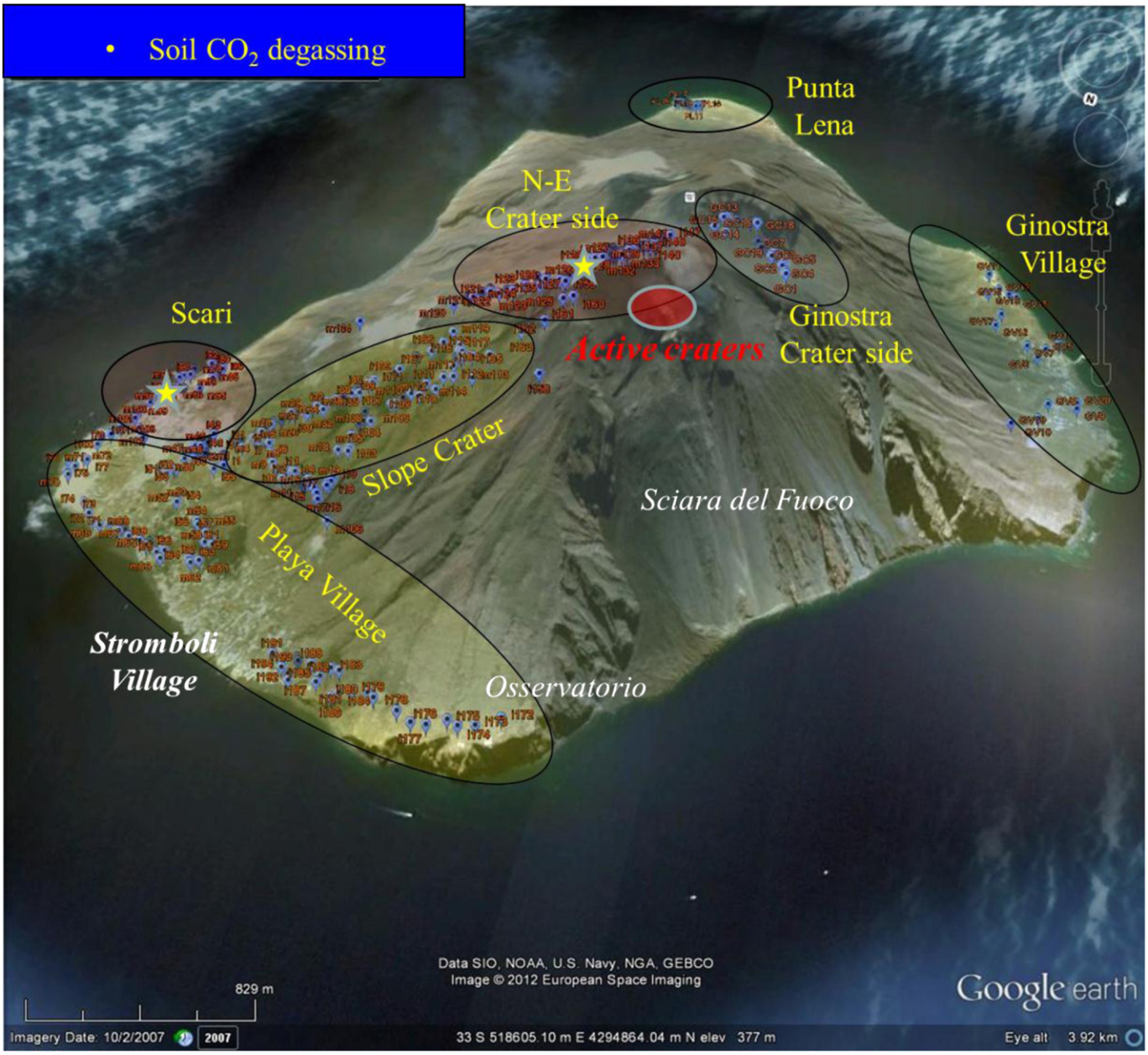

Fig. 1. Satellite view of Stromboli Island (Aeolian Archipelago, Sicily-Italy). Location of the soil CO_2 flux measurements performed on the whole island, the exposed surface was divided into 7 areas with different measurement steps in relation to the degree of soil gas emissions. The yellow stars indicate the position of STR02 (Crater area) and STR01 (Scari area).

volcanic monitoring program of INGV Palermo. The CO_2 soil flux data were acquired on an hourly basis arriving directly, by modem GSM, at the acquisition Center of INGV-Palermo and forwarded directly to the Italian Civil Protection Center in Rome.

The main purpose of this work is the estimation of the total output of CO_2 emitted by the volcano considering the soil diffuse degassing fluxes and the CO_2 flux emitted by the plume. CO_2-plume emission was estimated utilizing an indirect methodology (Aiuppa et al., 2010; Inguaggiato et al., 2011a) on the basis of SO_2 flux measurements with an UV scanning DOAS equipment and C/S value measured directly in the plume with a homemade portable equipment arranged with double detector (IR and Electrochemical sensor). Moreover, on the basis of the soil degassing survey we want to confirm the existence of the highest degasification zones and to verify whether the conditions remain stable or move the soil geochemical network equipments to new highest degassing areas if these conditions are changed.

2. Soil degassing processes

Geochemical investigations carried out on volcanic areas demonstrate that the study of the variations of extensive parameters, like output of mass and energy, are very important to monitor the volcanic activity (Chiodini et al., 1998; Diliberto et al., 2002; Carapezza et al., 2004; Rizzo et al., 2009; Inguaggiato et al., 2011a, 2012).

The carbon dioxide emitted from the soils is one of the parameters utilized inside of the geochemical volcanic surveillance program in the world (Chiodini et al., 1998; Carapezza et al., 2004; Frondini et al., 2004; Werner and Cardellini, 2006; Favara et al., 2001; Inguaggiato et al., 2011a,b; Mazot et al., 2011). In fact the carbon dioxide represents the main component of the dry volcanic gases, making it possible to monitor these parameters also in the period of quiescence of an active volcano. Moreover, the estimation of the total output of a volcanic system gives us information on the amount of magma batch involved in the degassing processes.

The total flux measured from the soils represents the result of the diffusive and advective degassing processes. Lower values of Φ_{CO_2} are driven by diffusion processes and are proportional to concentration gradient expressed by the first law of Fick:

$$\Phi_d = -\nu D(dC/dx) \quad (e1)$$

where ν and D represent respectively the soil porosity and the diffusion coefficient. The sign minus indicates that the molecules move from point with high concentration to point with low concentration. On the contrary, high values of flux are driven by advective processes that involve a force like the pressure gradient dP/dx. The advective flux Φ_a is well described by Darcy law.

$$\Phi_a = -K/\mu(dP/dx) \quad (e2)$$

where K is the specific permeability of the soil and μ is the viscosity of the fluid.

In the geothermal and volcanic systems the total degassing flux of volatiles from the soils is the result of the combination of these two kinds of fluxes in a different percentage on the basis of the power of degassing.

Many methodologies have been utilized to measure the soil CO_2 fluxes starting from Lundegardh, 1926, mainly applied to investigate the fluxes of agrarian soils. Then, the methods of dynamic accumulation chamber (Reiners, 1968; Kucera and Kirkham, 1971), static accumulation chamber (Parkinson, 1981), static alkaline traps (Edwards, 1982; Cerling et al., 1991), CO_2 dynamic concentration (Gurrieri and Valenza, 1988) were realized.

The dynamic accumulation chamber, modified and adapted to measure soil CO_2 fluxes in geothermal and volcanic areas by Chiodini et al., 1998, represents the most utilized method by the scientific community both for general survey and for continuous geochemical monitoring in volcanic areas (Chiodini et al., 1996; Cardellini et al., 2003; Brusca et al., 2004; Carapezza et al., 2004; Chiodini et al., 2005; Inguaggiato et al., 2005; Pecoraino et al., 2005; Werner and Cardellini, 2006; Inguaggiato et al., 2011a; Mazot et al., 2011; Inguaggiato et al., 2012).

3. Methodologies

The soil CO_2 flux measurements were carried-out with the portable flux-meter based on the accumulation chamber method (Chiodini et al., 1998). The equipment (West Systems) utilized in this field campaign was equipped with a detector LI-COR infrared sensor for CO_2.

SO_2 flux measurements were carried out on the plume using Mini-DOAS instruments consisting of an USB2000 ultra-violet spectrometer (spectral range 245–400 nm, resolution about 0.7 nm, manufactured by Ocean Optics Inc.) and a vertically pointing telescope of 7 mrad fields of view with a circular-to-linear converter 4×200 μm fiber bundle, which connects the telescope to the fiber. A USB cable connects the spectrometer to a laptop computer, providing power and means of data transfer. A software control of the USB2000 was achieved using J-scripts executed in DOASIS software (http://crusoe.iup.uniheidelberg.de/urmel/doasis/download/), for saving and analyzing spectra, providing real time concentration readings. Geographic coordinates for each spectrum were obtained using a hand held GPS receiver. Details of the used DOAS routine and the flux calculations can be found in Galle et al. (2003).

Considering the morphology of Stromboli, and on the basis of the dominant wind direction, the measurements were carried out by performing several traverse measurements during the day (five traverse) from a boat moving beneath the plume.

The C/S ratio in the plume was measured with equipment built in the INGV Palermo laboratory. The system is equipped with two detectors:

- infrared spectrometer, to measure CO_2 concentration (Gascard NG, 0–3000 ppmVol, Edimburg Sensor Company) with onboard barometric Pressure correction in the range 800–1150 mbar;
- SO_2 electrochemical sensor (EZT3SH Range 0–50 ppm City Technology Company).

Both detectors have been calibrated with certified standards (respectively in the ranges 0–3000 and 0–50 ppm).

Plume measurements were carried out on the Stromboli summit area (Pizzo sopra la fossa) about 200 m from the craters rim. Two filters 0.45 μm were applied at the entrance of gas driven by a membrane pump Boxer Series S. C/S ratio was computed by the measured CO_2/SO_2 slope.

4. Field work

On the basis of the previous geochemical investigation of soil CO_2 diffuse degassing (Carapezza and Federico, 2000; Brusca et al., 2004) 419 measures of CO_2 flux, by the accumulation chamber method (West systems equipment), were carried out in July 2010. Fig. 1 shows the location of the soil flux measurements points distributed in the following selected areas, covering almost the whole surface of Stromboli: Beach Village, Scari, Slope Crater, North-East Crater, Ginostra Crater, Punta Lena, Ginostra Village. In Appendix 1, the GPS coordinates and the fluxes in $g/m^2/day$ of each soil measurement, have been reported. The Sciara del Fuoco area has not been investigated for safety reason (flank instability). The SO_2 plume flux and the C/S ratio of the was also measured in the same period respectively by the UV-MiniDOAS (making several traverses below the plume with a boat) and by a homemade equipment with double detector (IR and Electrochemical sensor) directly on the summit area.

5. Soil CO_2 degassing output

5.1. Probability distribution of the CO_2 flux data

The probability plot of the considered 419 data (Fig. 2), shows multi modal distribution consistent with the partial overlapping of three log-normal populations named B, C and H. On the basis of the Sinclair (1974) technique, mean log flux CO_2 values of 2.62, 0.8 and −0.36, standard deviations of 0.37, 0.48 and 0.87, and relative proportion of 0.14, 0.78 and 0.07, were computed for populations H, B and C, respectively. The mean flux CO_2 and the 95% confidence interval of the mean (David, 1977) are for population H 598 $g/m^2/day$ (482–786 $g/m^2/day$), for population B 11 $g/m^2/day$ (10–13 $g/m^2/day$) and for population C 3 $g/m^2/day$ (1.2–16 $g/m^2/day$).

The three-population percentages were checked and validated by combining the three populations in the proportion of 15% H, 78% B and 7% C at various levels of log CO_2 flux. Populations B and C,

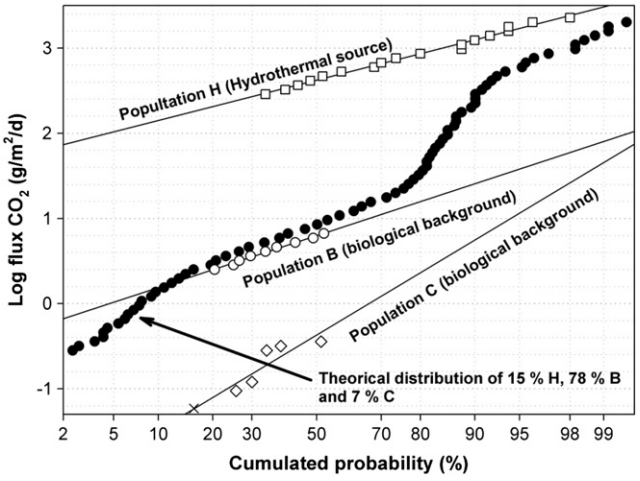

Fig. 2. Probability plot of the log flux CO_2. The data show a bimodal distribution with the partial overlapping of background populations (B and C) and the hydrothermal degassing (H).

representing low CO_2 flux, measured at all the sites of study, suggest that they both represent background levels, mainly controlled by biological CO_2 production in the soil. The difference between population B and C depends only on the permeability of the soil. Stromboli is covered by low permeability lava flows and the CO_2 flux measured being mostly relatively low in some areas.

5.2. Mapping and sequential Gaussian simulation (sGs) of the CO_2 flux from Stromboli

The distribution of degassing areas over Stromboli, and estimates of the total CO_2 discharged from the different areas, with associated errors, were derived by sequential Gaussian simulation (sGs) (Deutsch and Journel, 1998). (Fig. 2; Table 1). The density of the point measurement was increased in the areas with major degassing as suggested by the previous investigation.

5.2.1. N-E crater side

The 57 CO_2 fluxes measured in randomly distributed points on the Crater surface (Fig. 3) were interpolated by a distribution over a grid of 4186 square cells (8×8 m^2) covering an area of 67,500 m^2 using a exponential variogram model (Deutsch and Journel, 1998). Then, 100 simulations of the CO_2 fluxes with the obtained distribution were performed. For each simulation, the CO_2 flux estimated at each cell is multiplied by 68 m^2 and added to the other CO_2 fluxes estimated at the other cells of the grid to obtain a total CO_2 output for the simulation. The mean of the 100 total simulated CO_2 outputs, 26 t/day, represents the estimation of the total CO_2 output from the Crater area with a standard deviation of 1.35 t/day.

5.2.2. Beach village area

The 98 CO_2 fluxes measured in randomly distributed points on the Playa village (Fig. 3) area were interpolated by a distribution over a grid of 11,211 square cells (7×7 m^2) covering an area of 227,300 m^2. The mean of the 100 total simulated CO_2 outputs, 2 t/day, represents the estimation of the total CO_2 output from the Playa Village area with a standard deviation of 0.06 t/day.

5.2.3. Scari area

The 69 CO_2 fluxes measured in randomly distributed points on the Scari area (Fig. 3) were interpolated by a distribution over a grid of 7548 square cells (8×8 m^2) covering an area of 136,400 m^2. The mean of the 100 total simulated CO_2 outputs, 8.6 t/day, represents the estimation of the total CO_2 output from the Scari area with a standard deviation of 0.82 t/day.

5.2.4. Slope crater area

The 129 CO_2 fluxes, measured in randomly distributed points on the Slope crater surface (Fig. 3), were interpolated by a distribution over a grid of 8736 square cells (14×14 m^2) covering an area of 659,900 m^2. The mean of the 100 total simulated CO_2 outputs, 6 t/day, represents the estimation of the total CO_2 output from the Subida crater area with a standard deviation of 0.29 t/day.

5.2.5. Punta Lena area

The 19 CO_2 fluxes measured in randomly distributed points on the Punta Lena area were estimated by the mean of the data. The area covered was 2381 m^2. The mean of the CO_2 flux, 0.03 t/day, represents the estimation of the total CO_2 output from the Punta Lena area with a standard deviation of 0.003 t/day.

5.2.6. Ginostra crater side

The 20 measured CO_2 fluxes in randomly distributed points on the Ginostra Crater area were estimated by the mean of the data. The area covered was 17,389 m^2. The mean of the CO_2 flux, 0.4 t/day, represents the estimation of the total CO_2 output from the Ginostra Crater area with a standard deviation of 0.024 t/day.

5.2.7. Ginostra Village area

The 20 measured CO_2 fluxes in randomly distributed points on the Ginostra Village area were estimated by the mean of the data. The area covered was 171,219 m^2. The mean of the CO_2 flux, 2.4 t/day, represents the estimation of the total CO_2 output from the Ginostra Village area with a standard deviation of 0.2 t/day.

6. Plume degassing

The summit crater area of Stromboli Island is characterized by a continuous passive and active plume degassing from the main open conduct craters. The estimation of CO_2 output discharged by plume degassing was carried out by the indirect method (McGonigle et al., 2008; Aiuppa et al., 2010; Inguaggiato et al., 2011a,b, 2012) based on plume SO_2 flux measurements and their CO_2/SO_2 ratios.

The average SO_2 flux, measured during July 2010, was of 110 t day$^{-1}\pm20$. This value is comparable with the average fluxes measured by other authors (around 200 t day$^{-1}\pm50$) during the "normal" Strombolian activity (Aiuppa et al., 2010; Inguaggiato et al., 2011a,b).

The average of CO_2/SO_2 molar ratio value (5 ± 1) was carried-out on the basis of 4 plume measurements (around 20 min each), performed on the summit crater utilizing a CO_2/SO_2 instrument (see methodologies paragraph for details).

On the basis of the values of CO_2/SO_2 ratio (5 ± 1) and the SO_2 fluxes plume (110 t day$^{-1}\pm20$), we estimated a CO_2 flux discharged from the plume of about 370 t day$^{-1}\pm70$ by the following relation:

$$Q_{CO_2\ plume} = Q_{SO_2\ plume} * (CO_2/SO_2)_{plume}. \quad (e3)$$

7. Discussion and conclusion

A total CO_2 output of 416 t day^{-1} was estimated in July 2010 for the whole area of Stromboli Island considering the discharged fluids from soil degassing over the whole island (summit and peripheral areas), and from the active craters (plume). The main contribution to these degassing processes is represented by the fluids discharged from the summit area (396 t day^{-1}), with 370 and 26 t day^{-1} from active craters (plume) and crater soil degassing areas, respectively. The soil gas emissions from

Table 1
CO_2 flux estimated for single area; the density of point measurements for area is also reported.

Study area	Number of samples	Area (m^2)	Mean CO_2 flux (g/m^2/day)	Standard deviation	Total CO_2 output (t/day)	Standard deviation
Beach Village	98	227,300	10	0.3	2.3	0.06
Scari	69	136,400	63	6.0	8.6	0.82
Slope Crater	129	659,900	9	0.4	5.9	0.29
North-East Crater	57	67,500	381	20.0	26	1.35
Punta Lena	19	2381	11	1.1	0.03	0.003
Ginostra Crater	20	17,389	20	1.4	0.37	0.02
Ginostra Village	20	171,219	14	1.2	2.4	0.20

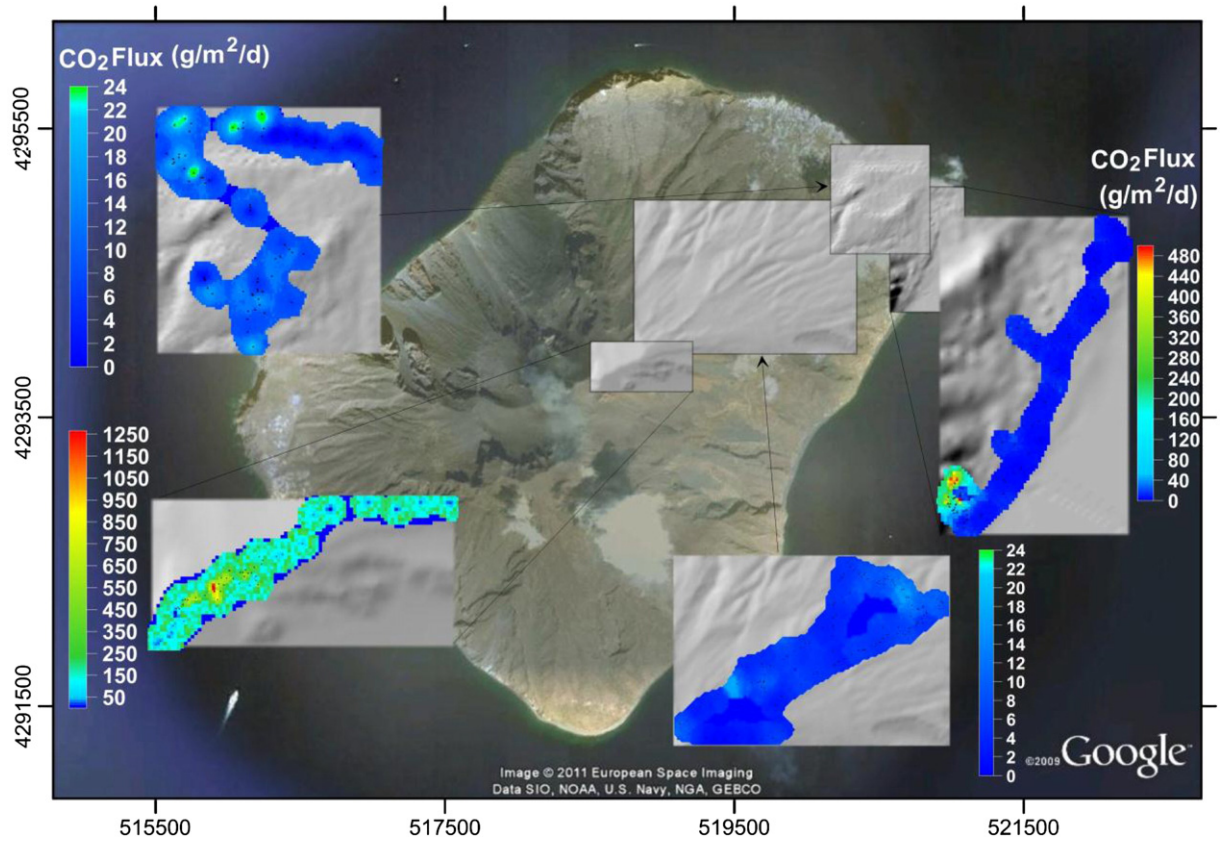

Fig. 3. CO_2 fluxes maps for the Stromboli Island.

peripheral areas, with respect to the active cone, were about 20 t day^{-1} of CO_2, mainly from the Scari and Slope Crater areas. This last survey highlights that the summit area represents more than 90% of the total CO_2 output of the entire island confirming that the monitoring of the fluids discharged from the summit area is the best way for following the changes of the volcanic activity (Inguaggiato et al., 2011a,b). We compare these results with other volcanic systems where the CO_2 peripheral and summit degassing have been estimated. In the graph of Fig. 4 we observe that open system degassing volcanoes like Popo and Etna, confirm the same behavior with CO_2 summit degassing one order of magnitude higher compared with the CO_2 peripheral degassing. While, closed system degassing volcanoes with solphataric activity like Ischia and Pantelleria islands, show an opposite behavior with CO_2 summit degassing one order of magnitude lower than the CO_2 peripheral degassing. Vulcano Island, although is a closed system volcano with solphataric activity, behaves like an open conduct volcano showing higher CO_2 summit

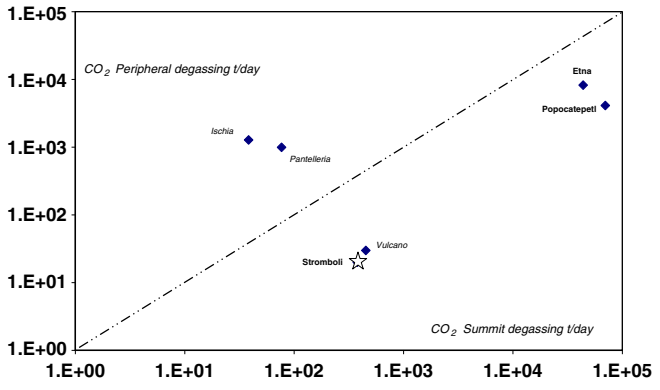

Fig. 4. CO_2 summit vs peripheral degassing for Stromboli Island (star symbol) compared with other open and closed volcanic systems. The CO_2 flux values are expressed in t/day.

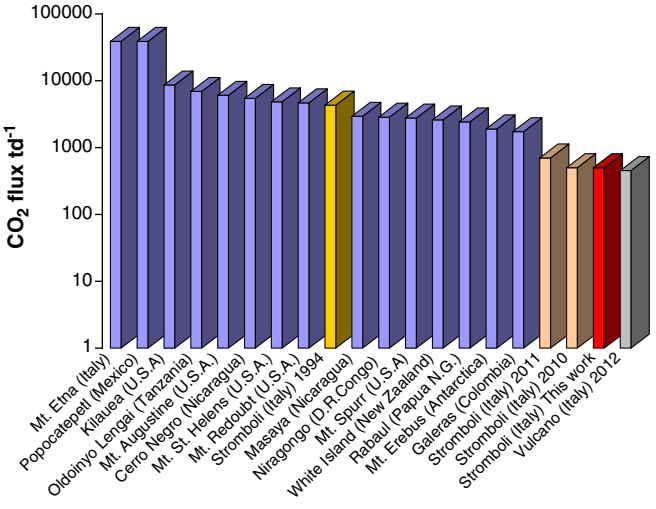

Fig. 5. Total CO_2 output released from Stromboli Island compared with other open conduct systems (i.e. Popocatépetl, Etna, etc.). Three plume CO_2 estimation was also reported (yellow and brown colors respectively for Allard et al., 1994; Aiuppa et al., 2010, Inguaggiato et al., 2011a,b). The CO_2 output estimation for Vulcano Island located in the same archipelago has been also reported for comparison (Inguaggiato et al., 2012). Mt. Etna (Italy), 38,880 t day^{-1}, D'alessandro et al. (1997); Popocatepetl (Mexico), 38,880 t day^{-1}, Goff et al. (2001); Kilauea (U.S.A.),8640 t day^{-1}, Gerlach et al. (2002); Oldoinyo Lengai (Tanzania),6912 t day^{-1},Braentley and Koepenick (1995) ; Mt. Augustine (U.S.A.), 6048 t day^{-1}, Symonds et al. (1992) ; Cerro Negro (Nicaragua), 5443 t day^{-1},Salazar et al. (2000) ; Mt. St. Helens (U.S.A.),4838 t day^{-1}, Harris et al. (1981) ; Mt. Redoubt (U.S.A.), 4666 t day^{-1},Hobbs et al. (1991) ; Stromboli (Italy), 4320 t day^{-1}, Allard et al. (1994) ; Masaya (Nicaragua), 2938 t day^{-1},Burton et al. (2000) ; Niragongo (D.R. Congo) 2851 t day^{-1},Le Guern (1987) ;Mt. Spurr (U.S.A.),2765 t day^{-1}, Doukas (1995) ; White Island (New Zealand), 2592 t day^{-1}, Wardell et al. (2004); Rabaul (Papua N.G.), 2419 t day^{-1},Perez et al. (1998); Mt. Erebus (Antarctica), 1901 t day^{-1},Wardell et al. (2004); Galeras (Colombia), 1728 t day^{-1},Stix et al. (1997).

degassing. This behavior could be related to the summit fracture increase, occurred in the last decades, which accounts for the decrease of deep fluids escapes towards the peripheral areas.

The plume CO_2 output (370 t day^{-1}) of Stromboli Island, estimated in July 2010, was compared with previous estimation carried-out in the past. In particular, this value of 370 t day^{-1} is in the same order of magnitude of recent plume output estimations of 450 and 700 t day^{-1} carried out respectively by Aiuppa et al., 2010 and Inguaggiato et al. (2011a,b), for the normal Strombolian activity (Fig. 5). While, the plume output estimation of 4800 t day^{-1} (Allard et al., 1994) is consistent with anomalous summit degassing activity of Stromboli volcano like showed by Aiuppa et al. (2010) and Inguaggiato et al. (2011a,b).

The total values of CO_2 output of the degassing system of Stromboli Island were also compared with other open volcanic systems all over the world (Fig. 5). We observe that the Stromboli volcano (Aeolian Archipelago) is characterized by lower CO_2 fluxes (397 t day^{-1}) in comparison with the other open conduct volcanic systems (up to 38,000 t day^{-1}, Popocatepetl, Etna D'alessandro et al., 1997; Goff et al., 2001). Moreover, the total CO_2 output of Vulcano island (located in the same Archipelago) recently estimated by Inguaggiato et al. (2012) showed similar lower values (453 t day^{-1}), suggesting that the magma feeding the volcanoes of the subduction system of Aeolian archipelago is CO_2-poor during quiescent activity.

Finally, nevertheless in the last 10 years two effusive eruptions (2002 and 2007) occurred with the opening of fractures on the flanks of the volcano, the areas with great soil anomalous degassing are still located in the *Pizzo sopra La Fossa* and in the *Scari* areas where the geochemical monitoring network operates with two continuous CO_2 soil monitoring stations that were installed in 1999–2000 (Brusca et al., 2004; Inguaggiato et al., 2011a,b). The persistence of the anomalous degassing in these two areas, chosen in the past, encourages us to continue in this direction for the geochemical monitoring of the volcanic activity of Stromboli.

Acknowledgments

The authors would like to thank Lucio Cárdenas González for the help during the field-work and the anonymous reviewers for the useful suggestions. Funding for this work was provided by INGV and by the FIEL-Volcan project of FONCICYT number 93645.

Appendix 1

Study area	Latitude (UTM-WGS 84)	Longitude (UTM-WGS 84)	CO_2 flux g m^{-2} day^{-1}
a) Beach Village	520312	4294865	1
	520336	4294817	17
	520458	4294816	8
	520460	4294812	10
	520446	4294763	13
	520443	4294739	7
	520473	4294831	7
	520475	4294862	6
	520475	4294825	6
	520578	4294790	6
	520615	4294938	7
	520580	4294943	14
	520543	4294930	9
	520453	4295081	5
	520451	4295089	7
	520315	4295155	12
	520266	4295160	13
	520308	4295172	12
	520280	4295186	40
	520220	4295218	16
	520216	4295214	21
	520217	4295229	15
	520222	4295332	24
	520254	4295351	25
	520487	4295365	28
	520430	4295323	12
	520493	4295322	17
	520532	4295304	0
	520592	4295301	0
	520653	4295285	0
	520752	4295282	0
	520315	4294859	2
	520322	4294834	15
	520430	4294824	15
	520467	4294768	8
	520461	4294655	22
	520444	4294700	8
	520475	4294853	4
	520490	4294824	7
	520477	4294801	18
	520480	4294783	15
	520496	4294757	8
	520518	4294870	13
	520572	4294952	12
	520557	4294966	6
	520530	4294924	13
	520453	4295071	2
	520327	4295162	3
	520302	4295172	8
	520251	4295199	9
	520254	4295239	18
	520236	4295243	20
	520234	4295233	17
	520661	4294330	63
	520651	4294297	38
	520653	4294284	23
	520652	4294270	3
	520646	4294262	3
	520689	4294280	3
	520751	4294340	9
	520753	4294378	1
	520797	4294410	1
	520819	4294451	5
	520781	4294474	21
	520830	4294526	4
	520863	4294590	2
	520892	4294637	18
	520890	4294672	12
	520929	4294764	5
	520957	4294810	10
	521056	4295060	0
	521078	4295001	0
	520999	4294977	0
	520993	4294873	5
	520617	4294328	184
	520620	4294368	451
	520618	4294298	66
	520608	4294313	218
	520616	4294295	91
	520613	4294295	18
	520605	4294305	346
	520601	4294314	605
	520602	4294332	314
	520616	4294327	94
	520645	4294293	43
	520654	4294271	20
	520644	4294248	26
	520692	4294286	4
	520755	4294372	7
	520781	4294396	2
	520852	4294485	1
	520750	4294480	8
	520848	4294537	5
	520901	4294679	1
	520929	4294772	3
	520993	4294837	2
	520840	4294742	6
	520790	4294789	9
b) Scari	521037	4295072	6
	521029	4295023	11

(continued on next page)

Appendix 1 (*continued*)

Study area	Latitude (UTM-WGS 84)	Longitude (UTM-WGS 84)	CO_2 flux g m^{-2} day^{-1}
	521013	4294970	4
	520620	4294330	805
	520625	4294377	997
	520659	4294325	88
	520623	4294311	203
	520622	4294310	168
	520618	4294289	54
	520626	4294290	34
	520620	4294303	34
	520634	4294324	1011
	520634	4294336	194
	520634	4294336	212
	520635	4294342	118
	520641	4294355	55
	519997	4294885	12
	519973	4294842	5
	519951	4294859	9
	519871	4294904	11
	519884	4294871	8
	519839	4294898	5
	519790	4294939	5
	519753	4294741	2
	519749	4294877	5
	520306	4294735	4
	520195	4294720	9
	520213	4294681	6
	520198	4294668	11
	520193	4294627	11
	520165	4294628	6
	520156	4294611	9
	520124	4294598	7
	520098	4294560	6
	520056	4294601	4
	519992	4294558	6
	519970	4294601	7
	519936	4294510	4
	519908	4294495	6
	519868	4294477	6
	519836	4294474	3
	519836	4294474	2
	519798	4294453	2
	519777	4294429	2
	519722	4294410	1
	519792	4294794	11
	519745	4294772	6
	519699	4294726	5
	519694	4294654	2
	519688	4294551	2
	519637	4294601	1
	519540	4294514	6
	519480	4294469	3
	519439	4294439	6
	519369	4294444	3
	519215	4294382	3
	519304	4294383	7
	519297	4294396	3
	519290	4294302	63
	519279	4294295	1
	519307	4294297	3
	519375	4294166	1
	519420	4294027	2
	519333	4294000	5
	520274	4294757	20
	520164	4294704	7
	520127	4294662	13
	520102	4294769	17
	520087	4294813	20
c) Slope crater	520297	4294744	9
	520194	4294714	7
	520166	4294701	16
	520132	4294722	24
	520113	4294766	15
	520075	4294814	17
	520036	4294837	14
	520023	4294863	12
	520032	4294851	17

Appendix 1 (*continued*)

Study area	Latitude (UTM-WGS 84)	Longitude (UTM-WGS 84)	CO_2 flux g m^{-2} day^{-1}
	520084	4294850	14
	519955	4294845	9
	519940	4294849	10
	519867	4294894	11
	519854	4294883	11
	519809	4294921	6
	519775	4294965	6
	519753	4294900	5
	519739	4294881	4
	519733	4294862	4
	520286	4294721	22
	520286	4294705	9
	520212	4294686	9
	520188	4294647	17
	520193	4294627	7
	520157	4294621	8
	520115	4294595	8
	520113	4294580	8
	520084	4294564	10
	520052	4294567	10
	520001	4294562	7
	519971	4294539	4
	519953	4294521	3
	519958	4294517	5
	519927	4294497	4
	519873	4294477	5
	519860	4294473	4
	519695	4294467	4
	519758	4294426	2
	519728	4294411	2
	519703	4294394	4
	519703	4294741	5
	519711	4294669	2
	519695	4294610	5
	519692	4294599	5
	519564	4294515	5
	519516	4294488	4
	519437	4294488	28
	519422	4294423	8
	519348	4294389	5
	519316	4294339	5
	519311	4294300	17
	519312	4294305	28
	519314	4294264	13
	519297	4294270	18
	519319	4294239	2
	519360	4293985	35
	519297	4293977	1
	519253	4293985	2
	519163	4294002	0
	519093	4293972	0
	518586	4293789	174
	518566	4293768	85
	518563	4293758	1
	518564	4293752	0
	518583	4293738	75
	518551	4293702	11
	518529	4293692	12
	518519	4293684	8
	518570	4293771	78
	518661	4293789	2023
	518653	4293808	1006
	518668	4293808	568
	518723	4293843	859
	518732	4293850	609
	518740	4293851	207
	518750	4293843	74
	518750	4293833	41
	518737	4293821	62
	518712	4293826	121
	520197	4295245	6
	520272	4295337	13
	520267	4295313	13
	520430	4295340	22
	520415	4295321	23
	520399	4295324	26

Appendix 1 (*continued*)

Study area	Latitude (UTM-WGS 84)	Longitude (UTM-WGS 84)	CO_2 flux g m^{-2} day^{-1}
	520487	4295299	3
	520564	4295288	1
	520623	4295283	1
	520649	4295262	3
	520703	4295263	2
	520788	4295270	0
	520833	4295237	3
	520833	4295189	4
	518683	4295692	4
	518776	4295745	9
	518843	4295766	6
	518891	4295753	9
	518970	4295792	14
	519033	4295798	15
	519103	4295769	8
	519216	4295740	7
	519247	4295727	15
	519315	4295730	5
	519401	4295667	6
	519437	4295663	6
	519372	4295748	5
	519372	4295702	3
	519400	4295770	10
	519486	4295727	4
	519533	4295660	12
	519595	4295648	15
	519618	4295718	11
	519720	4295651	13
	519608	4295744	4
	519658	4295699	10
	519659	4295672	3
d) North-East crater	519037	4293972	0
	518991	4293986	0
	518895	4294008	11
	518844	4294064	32
	518884	4294080	3
	518957	4294159	1
	519037	4294201	3
	519161	4294286	421
	519242	4294293	3
	519407	4294218	2
	519453	4294257	5
	519516	4294284	9
	519586	4294341	5
	519606	4294352	4
	519703	4294384	8
	519201	4294012	1
	519133	4294015	1
	519078	4293998	1
	519010	4294014	1
	518923	4293998	0
	518798	4293889	28
	518758	4293888	118
	518767	4293880	335
	518746	4293864	527
	518720	4293852	518
	518690	4293856	237
	518688	4293856	603
	518755	4293823	689
	518676	4293822	457
	518654	4293807	1581
	518654	4293808	5011
	518632	4293798	421
	518581	4293788	38
	518582	4293777	629
	518573	4293767	804
	518573	4293767	125
	518561	4293750	557
	518563	4293734	100
	518559	4293728	23
	518555	4293713	13
	518884	4293985	13
	518858	4293918	13
	518812	4293893	31
	518763	4293871	139
	518726	4293858	195

Appendix 1 (*continued*)

Study area	Latitude (UTM-WGS 84)	Longitude (UTM-WGS 84)	CO_2 flux g m^{-2} day^{-1}
	518714	4293852	336
	518698	4293837	348
	518683	4293838	993
	518670	4293839	903
	518664	4293825	876
	518651	4293820	2158
	518611	4293793	1443
	518592	4293788	1251
	518755	4291663	3
	518867	4291634	11
	518867	4291646	17
	518878	4291660	8
e) Punta Lena	518884	4291606	7
	518872	4291610	4
	518873	4291617	7
	518865	4291627	8
	518849	4291624	15
	518839	4291626	17
	518824	4291636	15
	518810	4291642	10
	518796	4291649	9
	518782	4291656	11
	518769	4291658	6
	518754	4291652	9
	518754	4291640	15
	518734	4291654	12
	518723	4291640	19
f) Ginostra crater	518000	4293641	27
	518003	4293629	12
	518016	4293593	9
	518024	4293600	22
	518019	4293581	24
	518044	4293559	12
	518072	4293540	20
	518118	4293518	28
	518114	4293489	27
	518152	4293494	12
	518205	4293429	15
	518264	4293433	21
	518325	4293439	24
	518302	4293497	26
	518311	4293435	12
	518354	4293491	18
	518132	4293527	19
	518175	4293427	23
	518079	4293559	20
g) Ginostra Village	516576	4293019	10
	516565	4292994	13
	516572	4293024	25
	516575	4293044	11
	516648	4293097	12
	516692	4293181	9
	516748	4293127	15
	516640	4293491	11
	516505	4293478	12
	516692	4293614	9
	516954	4292638	14
	516903	4292757	11
	516805	4292763	12
	516838	4292725	14
	516847	4292766	12
	516960	4292826	13
	516887	4292953	12
	516921	4293071	9
	516820	4293694	15
	516498	4293430	30

References

Aiuppa, A., Burton, M., Caltabiano, T., Giudice, G., Gurrieri, S., Liuzzo, M., Murè, F., Salerno, G., 2010. Unusually large magmatic CO_2 gas emissions prior to a basaltic paroxysm. Geophysical Research Letters 37, L17303 http://dx.doi.org/10.1029/2010GL043837.

Allard, P., Carbonnelle, J., Métrich, N., Loyer, H., Zettwoog, P., 1994. Sulphur output and magma degassing budget of Stromboli volcano. Nature 368, 326–330.

Barberi, F., Rosi, M., Sodi, A., 1993. Volcanic hazard assessment at Stromboli based on review of historical data. Acta Vulcanologica 3, 173–187.

Bertagnini, A., Métrich, N., Francalanci, L., Landi, P., Tommasini, S., Conticelli, S., 2008. In: Calvari, S., Inguaggiato, S., Puglisi, G., Ripepe, M., Rosi, M. (Eds.), The Stromboli Volcano: An Integrated Study of the 2002-2003 Eruption American Geophysical Union, 19–37.

Brantley, S., Koepenick, K., 1995. Measured carbon dioxide emissions from Oldoinyo Lengai and the skewed distribution of passive volcanic fluxes. Geology 23, 933–936.

Brusca, L., Inguaggiato, S., Longo, M., Madonia, P., Maugeri, R., 2004. The 2002–2003 eruption of Stromboli (Italy): evaluation of the volcanic activity by means of continuous monitoring of soil temperature, CO_2 flux, and meteorological parameters. Geochemistry, Geophysics, Geosystems http://dx.doi.org/10.1029/2004GC000732 (ISSN: 1525-2027).

Burton, M., Allard, P., Muré, F., La Spina, A., 2007. Magmatic gas composition reveals the source depth of slug-driven Strombolian explosive activity. Science 317, 227 http://dx.doi.org/10.1126/science.1141900.

Burton, M.R., Oppenheimer, C., Horrocks, L.A., Francis, P.W., 2000. Remote sensing of CO_2 and H_2O emission rates from Masaya volcano, Nicaragua. Geology 28 (10), 915–918.

Capasso, G., Carapezza, M.L., Federico, C., Inguaggiato, S., Rizzo, A., 2005. Geochemical monitoring of the 2002–2003 eruption at Stromboli volcano (Italy): precursory changes in the carbon and helium isotopic composition of fumarole gases and thermal waters. Bulletin of Volcanology 68, 118–134.

Carapezza, M.L., Federico, C., 2000. The contribution of fluid geochemistry to the volcano monitoring of Stromboli. Journal of Volcanology and Geothermal Research 95, 227–245.

Carapezza, M.L., Inguaggiato, S., Brusca, L., Longo, M., 2004. Geochemical precursors of the activity of an open-conduit volcano: the Stromboli 2002–2003 eruptive events. Geophysical Research Letters 31, L07620 http://dx.doi.org/10.1029/2004GL019614.

Cardellini, C., Chiodini, G., Frondini, F., 2003. Application of stochastic simulation to CO_2 flux from soil: Mapping and quantification of gas release. Journal of Geophysical Research 108, 2425 http://dx.doi.org/10.1029/2002JB002165.

Cerling, T.E., Solomon, D.K., Quade, J., Bowman, J.R., 1991. On the isotopic composition of carbon in soil carbon dioxide. Geochimica et Cosmochimica Acta 55, 3403–3405.

Chiodini, G., Cioni, R., Guidi, M., Raco, B., Marini, L., 1998. Soil CO_2 flux measurements in volcanic and geothermal areas. Applied Geochemistry 13, 543–552.

Chiodini, G., Frondini, F., Raco, B., 1996. Diffuse emission of CO_2 from the Fossa crater, Vulcano Island (Italy). Bulletin of Volcanology 58, 41–50.

Chiodini, G., Granieri, D., Avino, R., Caliro, S., Costa, A., Werner, C., 2005. Carbon dioxide diffuse degassing and estimation of heat release from volcanic and hydrothermal systems. Journal of Geophysical Research 110, B08204 http://dx.doi.org/10.1029/2004JB003542.

D'Alessandro, W., Giammanco, S., Parello, F., Valenza, M., 1997. CO_2 output and $\delta^{13}(CO_2)$ from Mount Etna as indicators of degassing of shallow asthenosphere. Bulletin of Volcanology 58, 455–458.

David, M., 1977. Geostatistical ore reserve estimation. Developments in Geomathematics, 2. Elsevier, New-York . (363 pp.).

Deutsch, C.V., Journel, A.G., 1998. GSLIB: Geostatistical Software Library and Users Guide, 2nd ed., Oxford Univ Press, New York, pp. 369.

Diliberto, I.S., Gurrieri, S., Valenza, M., 2002. Relationships between diffuse CO_2 emissions and volcanic activity on the island of Vulcano (Aeolian Islands, Italy) during the period 1984–1994. Bulletin of Volcanology 64, 219–228.

Doukas, M.P., 1995. A compilation of sulfur dioxide and carbon dioxide emission-rate data from Cook Inlet volcanoes (Redoubt, Spurr, Iliama and Augustine), Alaska, during the period from 1990 to 1994. U.S. Geological Survey Open-File Rep. 95–55.

Edwards, N.T., 1982. The use of soda-lime for measuring respiration rates in terrestrial systems. Pedobiologia 23, 321–330.

Favara, R., Giammanco, S., Inguaggiato, S., Pecoraino, G., 2001. Preliminary estimate of CO_2 output from Pantelleria Island volcano (Sicily, Italy): evidence of active mantle degassing. Applied Geochemistry 16, 883–894.

Frondini, F., Chiodini, G., Caliro, S., Cardellini, C., Granieri, D., Ventura, G., 2004. Diffuse CO_2 degassing at Vesuvio, Italy. Bulletin of Volcanology http://dx.doi.org/10.1007/s00445-004-0346-x.

Galle, B., Oppenheimer, C., Geyer, A., McGonigle, A.J.S., Edmonds, M., Horrocks, L.A., 2003. A miniaturised ultraviolet spectrometer for remote sensing of SO_2 fluxes: a new tool for volcano surveillance. Journal of Volcanology and Geothermal Research 119, 241–254.

Gerlach, T.M., McGee, K.A., Elias, T., Sutton, A.J., Doukas, M.P., 2002. Carbon dioxide emission rate of Kilauea volcano: Implications for primary magma and the summit reservoir. Journal of Geophysical Research 107 (B9), 2189 http://dx.doi.org/10.1029/2001JB000407.

Goff, F., Love, S.P., Warren, R.G., Counce, D., Obenholzner, J., Siebe, C., Schmidt, S.C., 2001. Passive infrared remote sensing evidence for large, intermittent CO2 emissions at Popocatepetl volcano, Mexico. Chemical Geology 177, 133–156.

Gurrieri, S., Valenza, M., 1988. Gas transport in natural porous mediums: a method for measuring CO_2 flows from the ground in volcanic and geotherma areas. Rendiconti della Societa Italiana di Mineralogia e Petrologia 43, 1151–1158.

Harris, D.M., Sato, M., Casadevall, T.J., Rose, W.I., Bornhorst, T.J., 1981. Emission rates of CO_2 from plume measurements. U.S. Geological Survey Professional Paper 1250, 201–207.

Hobbs, P.V., Radke, L.F., Lyons, J.H., Ferek, R.J., Coffman, D.J., Casadevall, T.J., 1991. Airborne measurements of particle and gas emissions from the 1990 volcanic eruptions of Mount Redoubt. Journal of Geophysical Research 96 (D10), 18735–18752.

Inguaggiato, S., Martin-Del Pozzo, A.L., Aguayo, A., Capasso, G., Favara, R., 2005. Isotopic, chemical and dissolved gas constraints on spring water from Popocatépetl (Mexico): evidence of gas–water interaction magmatic component and shallow fluids. Journal of Volcanology and Geothermal Research 141, 91–108.

Inguaggiato, S., Rizzo, A., 2004. Dissolved helium isotope ratios in ground-waters: a new technique based on gas-water re-equilibration and its application to Stromboli volcanic system. Applied Geochemistry 19, 665–673.

Inguaggiato, S., Vita, F., Rouwet, D., Bobrowski, N., Morici, S., Sollami, A., 2011a. Geochemical evidence of the renewal of volcanic activity inferred from CO_2 soil and SO_2 plume fluxes: the 2007 Stromboli eruption (Italy). Bulletin of Volcanology http://dx.doi.org/10.1007/s00445-010-0442-z.

Inguaggiato, S., Calderone, L., Inguaggiato, C., Morici, S., Vita, F., 2011b. Dissolved CO_2 in natural waters: development of an automated monitoring system and first application to Stromboli Volcano (Italy). Annals of Geophysics http://dx.doi.org/10.4401/ag-5180.

Inguaggiato, S., Mazot, A., Diliberto, I.S., Inguaggiato, C., Madonia, P., Rouwet, D., Vita, F., 2012. Total CO_2 output from Vulcano island (Aeolian Islands, Italy). Geochemistry, Geophysics, Geosystems http://dx.doi.org/10.1029/2011GC003920 (ISN: 1525-2027).

Kucera, C.L., Kirkham, D.R., 1971. Soil respiration studies in tallgrass prairie in Missouri. Ecology 52, 912–915.

Lundegardh, H., 1926. Carbon dioxide evolution of soil crop growth. Soil Science 6, 417–453.

Le Guern, F., 1987. Mechanism of energy transfer in the lava lake of Niragongo (Zaire), 1959–1977. Journal of Volcanology and Geothermal Research 31, 17–31.

Mazot, A., Rouwet, D., Taran, Y., Inguaggiato, S., Varley, N., 2011. CO_2 and He degassing at El Chichón volcano (Chiapas, Mexico): gas flux, origin, and relationship with local and regional tectonics. Bulletin of Volcanology 73, 423–441 http://dx.doi.org/10.1007/s00445-010-0443-y.

McGonigle, A.J.S., Aiuppa, A., Giudice, G., Tamburello, G., Hodson, A.J., Gurrieri, S., 2008. Unmanned aerial vehicle measurements of volcanic carbon dioxide fluxes. Geophysical Research Letters 35, L06303.

Parkinson, K.J., 1981. An improved method for measuring soil respiration in the field. Journal of Applied Ecology 18, 221–228.

Pecoraino, G., Brusca, L., D'Alessandro, W., Giammanco, S., Inguaggiato, S., Longo, M., 2005. Total CO_2 output from Ischia Island volcano (Italy). Geochemical Journal 39, 451–458 (special issue).

Perez, N.M., Nakai, S., Notsu, K., Talai, B., 1998. Anomalous diffuse degassing of helium-3 and CO_2 related to the active Ring-Fault structure at Rabaul Caldera, Papua New Guinea. EOS Trans. AGU 79 (45) Fall Meet. Suppl., F957.

Rosi, M., Bertagnini, A., Landi, P., 2000. Onset of the persistent activity at Stromboli Volcano (Italy). Bulletin of Volcanology 62, 294–300.

Reiners, W.A., 1968. Carbon dioxide evolution from the floor of three Minnesota forest. Ecology 49, 471–483.

Rizzo, A., Grassa, F., Inguaggiato, S., Liotta, M., Longo, M., Madonia, P., Brusca, L., Capasso, G., Morici, S., Rouwet, D., Vita, F., 2009. Geochemical evaluation of observed changes in volcanic activity during the 2007eruption at Stromboli (Italy). Journal of Volcanology and Geothermal Research 182, 246–254.

Salazar, M.L., Hernandez, P.A., Alvarez, J., Segura, F., Melian, G., Perez, N.M., Notzu, K., 2000. Diffuse emission of CO_2 from Cerro Negro volcano, Nicaragua, Central America. IAVCEI General Assembly 2000, Abstracts, July 18 –22, 2000, Bali, Indonesia.

Sinclair, A.J., 1974. Selection of threshold values in geochemical data using probability graphs. Journal of Geochemical Exploration 3, 129–149.

Stix, J., Calvache, V.M.L., Williams, S.N., 1997. Galeras volcano, Colombia: Interdisciplinary study of a decade volcano (special issue). Journal of Volcanology and Geothermal Research 77, 338.

Symonds, R.B., Reed, M.H., Rose, W.I., 1992. Origin, speciation, and fluxes of trace-element gases at Augustine volcano, Alaska: Insights into magma degassing and fumarolic processes. Geochimica et Cosmochimica Acta 56, 633–657.

Wardell, L.J., Kyle, P.R., Chaffin, C., 2004. Carbon dioxide and carbon monoxide emission rates from an alkaline intra-plate volcano: Mt. Erebus, Antarctica. Journal of Volcanology and Geothermal Research 131, 109–121.

Werner, C., Cardellini, C., 2006. Comparison of carbon dioxide emissions with fluid upflow, chemistry, and geologic structures at the Rotorua geothermal system, New Zealand. Geothermics 35, 221–238.